CONF-8508107--1

DAMAGE-RATE GRADIENT EFFECTS ON RADIATION-INDUCED SEGREGATION AND PHASE STABILITY IN IRRADIATED ALLOYS*

N. Q. Lam and P. R. Okamoto
Materials Science and Technology Division
Argonne National Laboratory
Argonne, Illinois 60439

CONF-8508107--1

DE85 016605

July 1985

Invited paper, to be presented at the "International Seminar on Solute Defect Interaction: Theory and Experiment", Kingston, Ontario, Canada, August 5-9, 1985.

*Work supported by the U. S. Department of Energy.

DAMAGE-RATE GRADIENT EFFECTS ON RADIATION-INDUCED SEGREGATION AND PHASE STABILITY IN IRRADIATED ALLOYS*

N. Q. Lam and P. R. Okamoto
Materials Science and Technology Division
Argonne National Laboratory
Argonne, Illinois 60439

July 1985

Invited paper, to be presented at the "International Seminar on Solute Defect Interaction: Theory and Experiment", Kingston, Ontario, Canada, August 5-9, 1985.
*Work supported by the U. S. Department of Energy.

DAMAGE-RATE GRADIENT EFFECTS ON RADIATION-INDUCED SEGREGATION AND PHASE STABILITY IN IRRADIATED ALLOYS

N. Q. Lam and P. R. Okamoto

Materials Science and Technology Division
Argonne National Laboratory
Argonne, Illinois 60439, USA

ABSTRACT

Recent studies have shown that significant compositional redistribution in irradiated alloys can be induced by the gradients in the atomic displacement rates resulting from nonuniform defect production, in addition to the commonly-observed solute segregation at defect sinks. This process gives rise to complex local phase transformations during light-ion bombardment or irradiation with focused electron beams in the high-voltage electron microscope. Results of our theoretical and experimental investigations of this phenomenon are discussed. The implications of the observed effect in a number of areas of materials science are assessed.

KEYWORDS

Radiation effects; radiation-induce segregation; phase stability; defect-solute interactions; proton bombardment; high-voltage electron-microscope irradiation.

INTRODUCTION

The relevance of radiation-induced phase instability to the engineering of materials used in irradiation environments, and the potential application of radiation-assisted modifications of subsurface alloy compositions have recently stimulated the search for a fundamental understanding of processes and mechanisms by which alloy phases are transformed during elevated-temperature irradiation.

The stable state of an alloy during its high-temperature service is generally known with the aid of existing phase diagrams or may, in principle, be predicted theoretically from thermodynamic criteria [1]. The alteration of the phase stability of alloys by irradiation is a new development, which can be encountered when materials are subjected to irradiation. A number of processes can give rise to the appearance of unexpected phases: (a) radiation-induced disordering of ordered phases [2], (b) recoil dissolution of thermodynamically-stable precipitates [3], (c) radiation-induced changes in free energies, and hence in the relative stability of phases [4], (d) radiation-enhanced diffusion, which significantly increases the rate of achieving phase equilibrium [5], and (e) radiation-induced segregation (RIS) of alloying elements [6-13]. Among these various

processes, RIS has been found to have a profound effect on the phase microstructure of alloys. This phenomenon causes significant compositional redistribution, effectively shifting local alloy compositions into different parts of the phase diagram. Thus, on a local scale, RIS tends to drive alloy systems away from thermodynamic equilibrium.

RIS results from the drift of solute atoms in a radiation-produced point-defect concentration gradient. In general, a gradient in vacancy or interstitial concentration gives rise to a flow of defects, with a corresponding flow of atoms. If solute atoms do not participate in this flow in proportion to their local concentration, e.g. because of defect-solute interactions, a net drift of solute atoms relative to the lattice planes will take place. During irradiation, the defect flow persists in time, thus local elemental concentration gradients will be set up and maintained. Strong local solute enrichment or depletion can result in precipitation of a new phase whenever the solute solubility is exceeded, or dissolution of a pre-existing phase, respectively. Persistent defect fluxes originate from the spatial nonuniformity in defect annihilation and/or defect production. Local elimination of point defects at extended sinks, such as dislocations, voids, grain boundaries and surfaces can induce them. Significant RIS and resulting precipitation of a new phase at these sinks have been routinely observed in many irradiated alloys [12,13]. Defect trapping at local inhomogeneities, such as solute clusters and coherent interfaces that enhance defect recombination, can also give rise to persistent defect fluxes [12]. Another cause is the gradient in the damage rates resulting from spatially-nonuniform defect production, e.g. during light-ion bombardment or irradiation with focused electron beams in the high-voltage electron microscope (HVEM) [8, 14-20]. The present paper focuses on the influence of displacement-rate gradients on the kinetics of RIS and its impact on phase destabilization in irradiated alloys. The implications of the observed effects in a number of areas of materials science are discussed.

RIS AND LOCAL PHASE INSTABILITY IN ION-BOMBARDED ALLOYS

The simplest demonstration of the damage-rate gradient effects on RIS can be taken from the experimental observations in ion-bombarded Ni-Si alloys. In this case, the gradients result from the one-dimensional nonuniformity in the defect production. This nonuniformity is more severe with light ions than with heavy ions. For example, as shown by the dotted curve in the left insert of Fig. 1 for 250-keV H^+ on Ni, the defect-production rate is small and virtually uniform in the near-surface region, but increases rapidly to a maximum value before dropping off to zero near the end of range. The peak rate is ~20 times larger than the near-surface rate. Consequently, defect fluxes that provide the driving forces for RIS are generated not only in the vicinity of defect sinks, including the bombarded surface, but also near the peak-damage depth where steep defect concentration gradients exist. The combination of defect fluxes near the surface and in the peak-damage region modifies the alloy phase microstructure in a peculiar fashion, as shown in Fig. 1 for a supersaturated Ni-12.7 at.% Si alloy irradiated at 550°C [21]. Presented here is a cross-sectional view of the bombarded zone showing local segregation-induced phase transformations. This type of phase instability can be interpreted as follows. Persistent defect fluxes in the alloy generated net fluxes of Si atoms in the same direction (Si has a preferential association with interstitials in Ni-Si alloys [13]) to the bombarded surface and out of the peak-damage region into the mid-range and beyond-range regions. Our theoretical calculations (Fig. 1, left insert), as well as experimental measurements [21], indicated that strong Si enrichment took place in those regions where there was a net influx of Si atoms, at the expense of severe Si depletion in the near-surface and peak-damage zones. In fact, the shape of the Si concentration

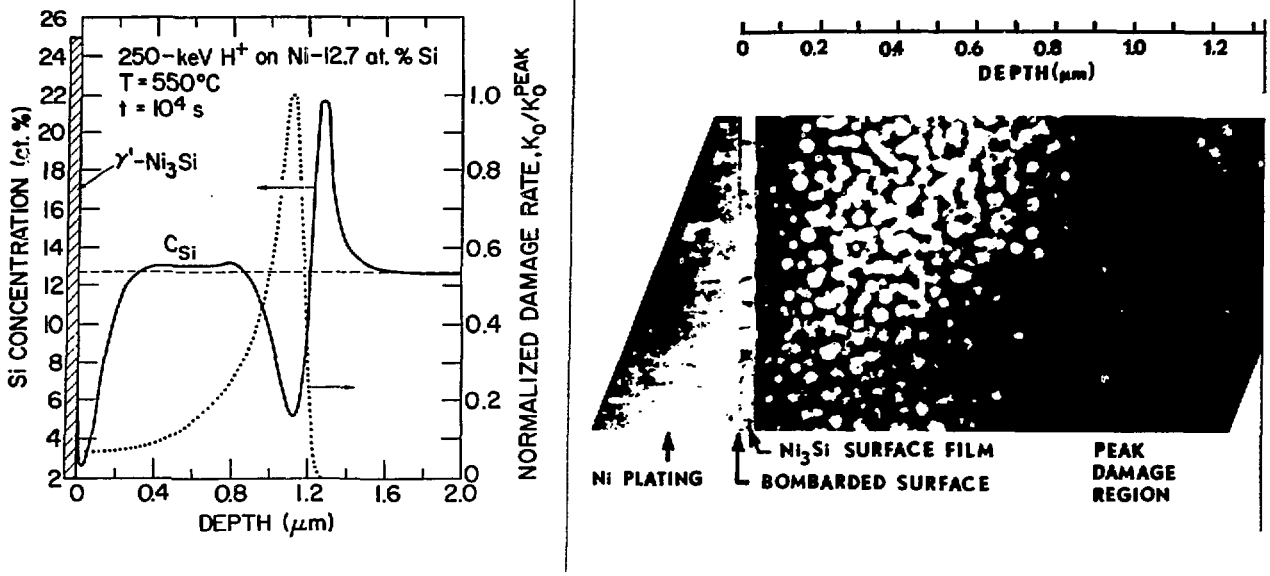

Fig. 1. Dark-field image, in cross section, of γ'-Ni_3Si precipitates formed in a Ni-12.7 at.% Si alloy bombarded with 250-keV H^+ at 550°C. The left insert illustrates the damage-rate distribution (dotted curve) and the Si concentration profile calculated using the physical parameters tabulated in ref. 17 (solid curve).

profile resembles the plot of the defect-flux divergence, because the rate of solute accumulation or depletion at a given depth, $\partial C_s/\partial t = -\nabla \cdot J_s$, is proportional to $\nabla^2 C_d$ (with d standing for vacancies or interstitials) [15]. As a result of local Si enrichment, a γ'-Ni_3Si precipitate film formed on the surface, and coherent γ' particles precipitated out in the mid-range and beyond-range regions. The measured spatial distribution of the γ' phase is in good agreement with the calculated Si redistribution profile. The same observations were also made in undersaturated Ni-Si solid solutions by Janghorban and Ardell [14,22].

RIS AND LOCAL PHASE INSTABILITY IN HVEM-IRRADIATED ALLOYS

During the past decade, the HVEM has been widely used to study the response of alloys to displacement damage. In order to reproduce in short times many of the high-dose effects observed in reactor-irradiated alloys, such as void formation, radiation-enhanced coarsening, and radiation-induced segregation and precipitation, HVEM irradiation experiments routinely employ highly-focused electron beams. Although such beams typically have a Gaussian flux distribution, and hence generate displacement-rate profiles that are radially nonuniform, it has traditionally been assumed that radial gradients in the displacement rate have no significant consequences on the kinetics of these processes. However, recent theoretical modeling [17,18] and experimental studies [18,19] indicate that such gradients can profoundly influence the kinetics of RIS in alloy films. Model calculations of two-dimensional RIS [17] have shown that the compositional redistribution induced by focused electron beams consists of two components. At relatively short irradiation times, axial segregation occurs at the film surfaces due to the proximity of these surfaces which act as defect sinks. Then, as the irradiation continues, radial segregation becomes important, gradually affecting the kinetics of axial segregation. The time scale for the occurrence of these components, and the competition between them depend on the beam characteristics,

e.g., the beam size relative to the film thickness. The average alloy composition in the irradiated zone can become drastically different from that of the unirradiated alloy, because of the atom transport from or to the region surrounding the irradiated zone under the influence of radial fluxes. As a result, radiation-induced formation of a new phase or disappearance of pre-existing phases may take place within the irradiated volume.

The beam-induced composition changes can be better understood in terms of the point-defect concentration gradients produced by the irradiation. As shown schematically in Fig. 2, the shape of the point-defect concentration profile in the radial direction will simply be a diffusion-broadened version of the beam intensity profile. During irradiation, the radial gradients induce a radial

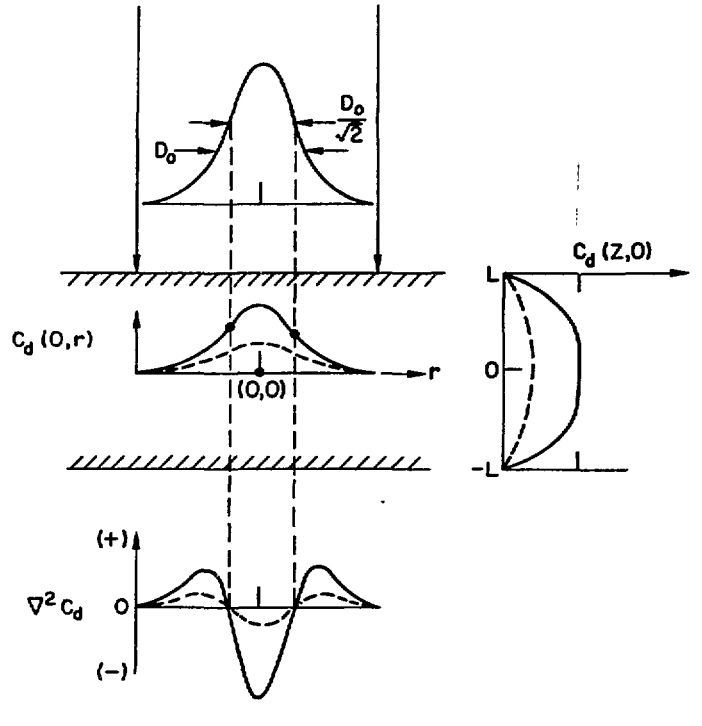

Fig. 2. Schematic illustration of spatial variations in defect concentration and defect-flux divergence in a thin film irradiated with a Gaussian beam. The dashed and solid curves are for thin and thick films, respectively.

flow of defects outward from the center of the beam. Due to the proximity of the foil surfaces, an axial flow of defects toward the surfaces will also occur. Both the radial and axial defect fluxes will in turn induce a net flow of solute atoms. The resulting solute concentration profile in the radial direction will resemble the radial variations in the point-defect flux divergence profile, $\nabla^2 C_d$, as discussed in the above section. When the fluxes of solute atoms and point defects are in opposite directions, as observed in, e.g., Ni-Al alloys, then solute enrichment will occur in regions where $\nabla^2 C_d$ is negative. The diameter of this region is equal to twice the standard deviation of the beam profile. Outside this central zone, where $\nabla^2 C_d$ is positive, a depletion in the Al concentration will occur. On the contrary, in alloys in which the solutes segregate in the same direction as the defect fluxes (e.g., in Ni-Si), solute enrichment will take place in regions where $\nabla^2 C_d$ is positive, and depletion will occur wherever $\nabla^2 C_d$ is negative.

Systematic experiments were carried out recently to demonstrate these effects of

radial displacement-rate gradients. A particularly striking example is presented in Fig. 3. This series of dark-field micrographs shows beam-induced changes occurring in an initially-uniform dispersion of γ'-Ni_3Al precipitates in a Ni-12.7 at.% Al alloy. The irradiation was carried out at 700°C using a focused beam of 1-MeV electrons. The effective diameter D_o shown by the circle at time zero is 0.64 μm, and the electron flux at the center of the beam was $5 \times 10^{19}/cm^2s$. During irradiation, Al atoms are drawn toward the center of the beam, causing rapid growth of precipitates within a central circular zone of approximately $0.7D_o$ in diameter. Outside this zone, precipitates become unstable and dissolve. The precipitate-free zone defines the region from which Al atoms are drained. Precipitates in this region dissolve when the Al concentration falls below the solubility limit of Al in Ni (11.6 at.% Al at 700°C [23]). The beam-induced changes in alloy composition can be sufficiently large to induce homogeneous precipitation in normally stable undersaturated solid solutions. This is demonstrated in Fig. 4 for a Ni-10 at.% Al alloy film irradiated at 700°C. The left insert of Fig. 4 shows the calculated time evolution of the Al concentrations at the foil surface and center, C^s_{Al} and C^c_{Al}, respectively, during irradiation [17,18]. After ~10^3s, C^c_{Al} starts to exceed the Al solubility limit. Thus, a new phase is expected to appear at this time and grow as the irradiation goes on. The experimental observations are shown by the micrographs in Fig. 4. Indeed, new γ'-Ni_3Al particles were formed in the beam center after ~900 s and then gradually spread outward within the irradiated area. The precipitates were not distributed uniformly in the axial direction, but, as predicted, were concentrated near the midplane of the foil where the surface sink effect is smallest.

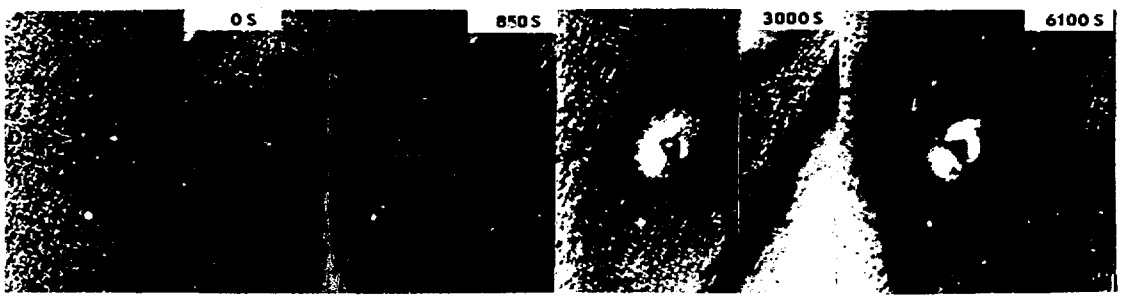

Fig. 3. Dark-field micrographs showing the evolution of the precipitate microstructure in a two-phase Ni-12.7 at.% Al alloy during irradiation at 700°C with 1-MeV electrons.

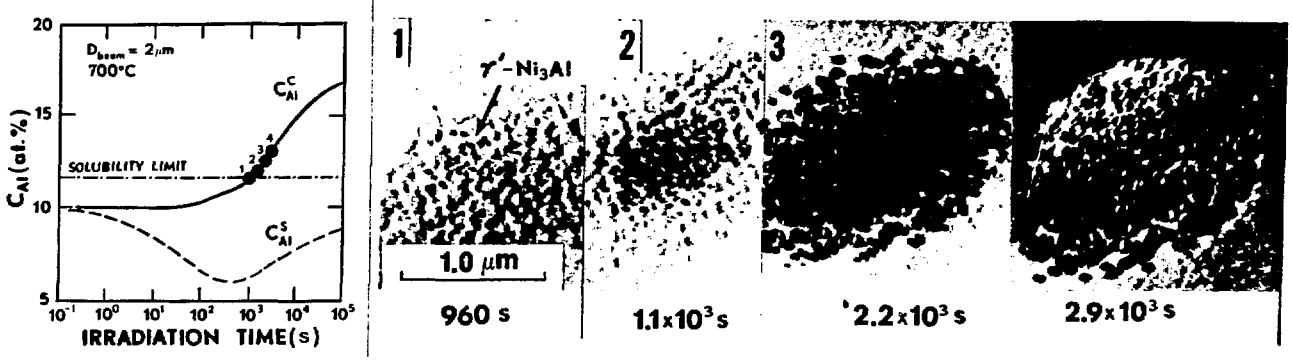

Fig. 4. Bright-field images showing the formation of coherent γ'-Ni_3Al precipitates within the irradiated zone in a Ni-10 at.% Al alloy irradiated with 1-MeV electrons at 700°C. The left insert shows the calculated time dependence of the Al concentrations at the surface and center of the foil.

An example of electron beam-induced phase instability in Ni-Si alloys is given in Fig. 5. Here, the RIS behavior is opposite to the one observed in the Ni-Al system, because the Si atoms and point defects diffuse in the same direction. After a few seconds of irradiation, a γ'-Ni_3Si precipitate film formed on each of the foil surfaces. It appeared first at the beam center and then grew radially outward to cover the entire irradiated area. Spatially, the surface γ'-film thickness was not uniform, it was maximum at the center and decreased in the radial direction to zero at the edge of the beam. Furthermore, as the irradiation continued, a ring of coherent γ' particles was observed near the edge of the irradiated zone. This ring is a characteristic feature of irradiations of alloys carried out with highly-focused beams and results from the effects of radial segregation. The appearance of this γ' ring is thus similar to the γ' precipitation observed in the mid-range and beyond-range regions of proton-bombarded Ni-Si alloys discussed in the above section. Radial segregation led to a severe depletion of Si in the center of the irradiated zone, which, in turn, induced back-diffusion of Si atoms from the surface regions. Consequently, for long irradiations, the surface γ' films gradually dissolved into the matrix and eventually disappeared.

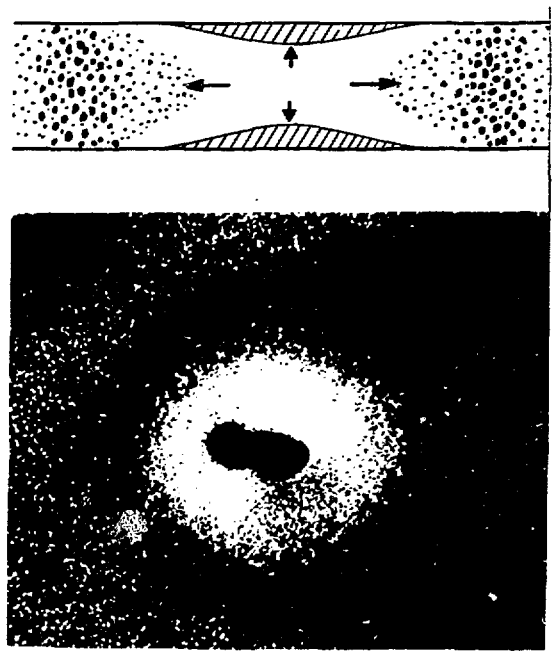

Fig. 5. Dark-field image showing local phase transformations in a two-phase Ni-12.7 at.% Si alloy foil irradiated with 1-MeV electrons at 600°C [24].

The mean diffusion length involved in the radial segregation process is the distance between the center of the beam, where $\nabla^2 C_d$ is a minimum, and the point where it attains its maximum value (see Fig. 2), i.e., the distance between regions of maximum enrichment and maximum depletion. This radial distance is approximately equal to the effective beam radius $0.5D_o$. Hence, at a given temperature, and for a fixed peak electron flux, the time required to produce a given change in alloy composition at the center of the beam should increase in proportion to the square of the beam diameter. To demonstrate this experimentally, the incubation time required to initiate precipitation of γ'-Ni_3Al particles in the center of the irradiated zone in a Ni-10 at.% Al alloy was measured as a function of beam diameter. The irradiations were carried out at 700°C, using fully-focused beams with beam conditions adjusted to maintain a constant peak electron flux of $5 \times 10^{19}/cm^2s$ for each beam diameter employed. The results are shown in Fig. 6. The measured incubation times indeed exhibit the expected parabolic dependence on beam diameter.

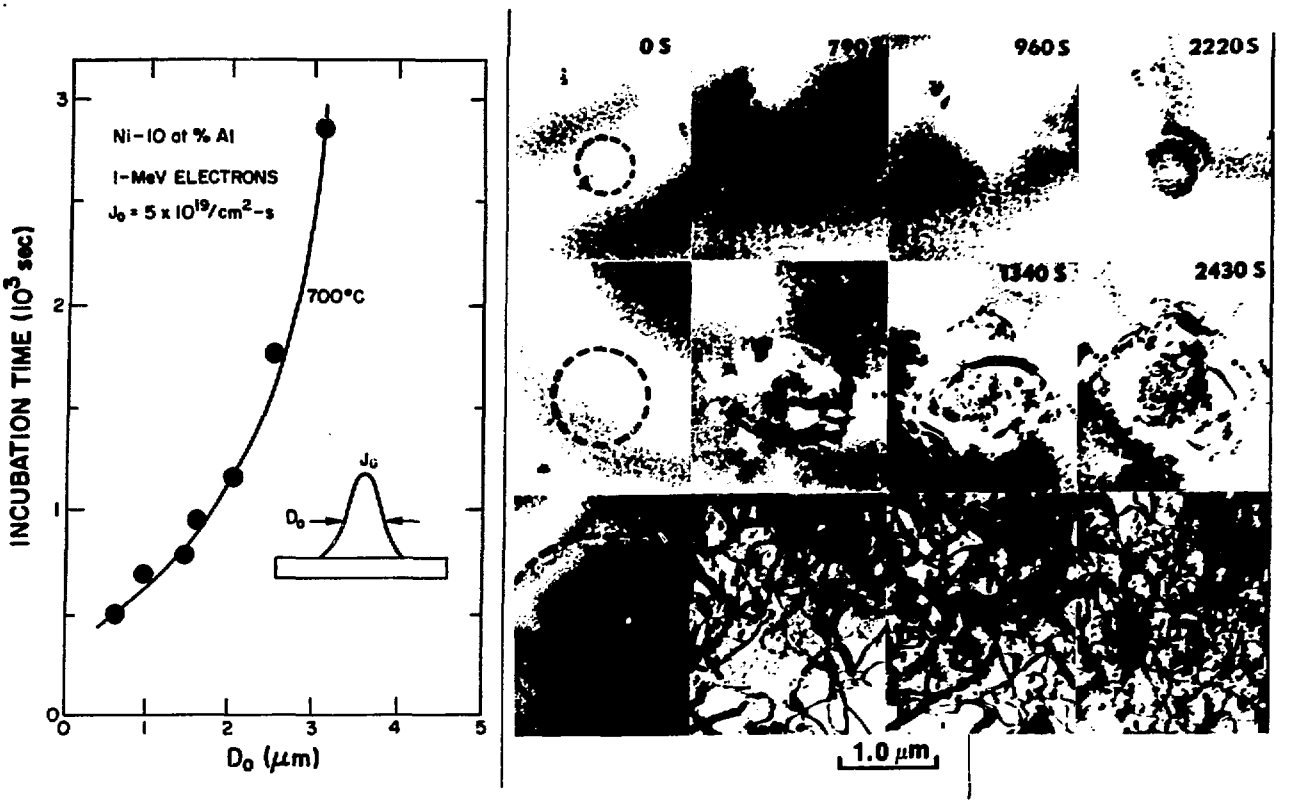

Fig. 6. Incubation times for beam-induced precipitation in a Ni-10 at.% Al alloy measured as a function of beam diameter. Some bright-field images showing the time evolution in the phase microstructure are included. The dashed circles indicate the effective beam sizes.

IMPLICATIONS OF THE DAMAGE-RATE GRADIENT EFFECTS

The present work demonstrates that the kinetics of RIS in a given alloy system depends not only on temperature, but also on the spatial characteristics of the damage-rate profile, since the defect fluxes that provide the basic driving forces for RIS are produced in any region where the damage rate changes rapidly. In the ion-bombardment case, such regions exist near the peak-damage depth in irradiated materials. Yet, it is precisely in this region, where the compositional changes due to RIS are expected to be quite severe, that experimental measurements of the damage structure (e.g. voids and dislocations) have most frequently been made. Unambiguous interpretations of these data will require a careful analysis of complex RIS effects. In the case of electron irradiation of thin alloy films, the dependence on beam size and shape poses a number of previously-unrecognized problems for in situ HVEM studies of radiation-induced phenomena sensitive to alloy composition. First, there is a problem in the interpretation of dose-rate effects. In practice, the dose-rate dependence is determined by measuring property changes as a function of the peak electron flux. However, it is difficult to obtain large changes in peak electron flux without also changing the beam diameter. Consequently, changes in kinetics resulting solely from changes in peak electron flux cannot be separated from displacement-rate gradient effects. In fact, it is doubtful whether the ordinary concept of a dose-rate dependence can retain its usual physical significance when highly-focused beams are employed to study composition-sensitive phenomena under conditions where displacement-rate gradients dominate the kinetics. Second, most quantitative studies of radiation-

enhanced coarsening have been carried out in the HVEM using highly-focused beams. The Ni-12.7 at.% Al alloy shown in Fig. 3 has frequently been used as a classic model system for such studies. The present work clearly shows that RIS driven by displacement-rate gradients will overwhelm simple radiation-enhanced coarsening processes. And third, focused beams have also commonly been employed for in situ HVEM studies of RIS at grain boundaries. The results have generally been interpreted in terms of compositional changes induced by defect flow to the grain boundary. However, when highly-focused beams are centered on the boundary, the radial defect fluxes generated by the beam will not only oppose the defect flux towards the boundary, but will also be larger in magnitude. As a consequence, the observed segregation may appear to contradict the expected behavior. An example is given in Fig. 7. Here, a zone containing a grain boundary in a supersaturated Ni-12.7 at.% Al sample, which had been pre-bombarded with 1-MeV protons at 525°C, was irradiated with a focused beam of 1-MeV electrons at 600°C. Before electron irradiation, radiation-induced coherent γ' particles were observed in the interior of grains and γ'-denuded zones formed on both sides of the grain boundary, consistent with previous observations that Al depletion was radiation-induced at defect sinks. However, this normal segregation behavior was completely changed by HVEM irradiation, as shown in Fig. 7. Radial RIS led to strong Al enrichment and, consequently, precipitation of the γ' phase at the grain boundary.

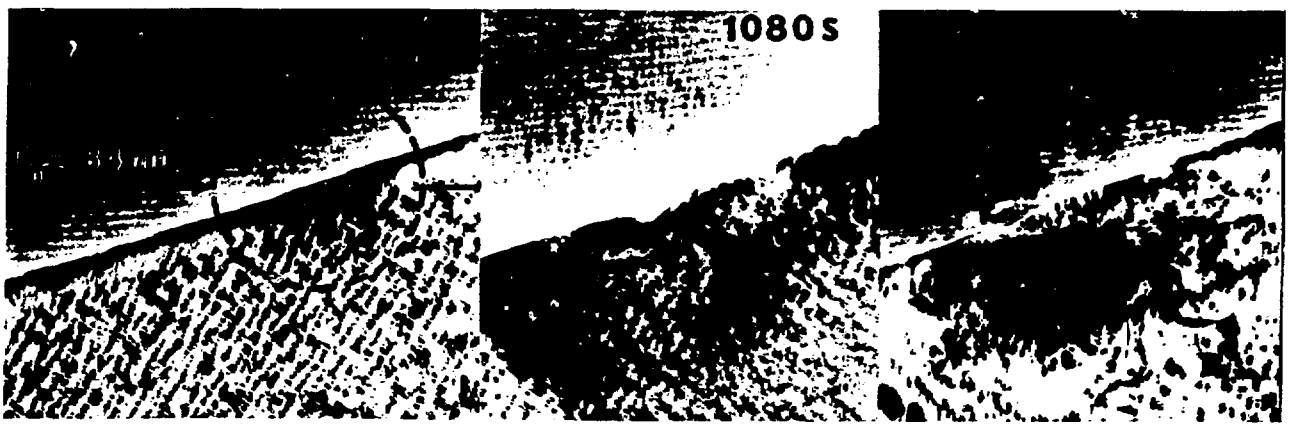

Fig. 7. Precipitation of the γ' phase at the grain boundary in a Ni-12.7 at.% Al alloy during 1-MeV electron irradiation at 600°C.

The implications of the present work extend beyond radiation effects per se. As shown in Fig. 6, composition changes driven by radial displacement gradients occur at increasingly rapid rates as the beam diameter is reduced. For example, the time required to increase the Al concentration in Ni-Al alloys by more than 20% is only a few hundred seconds as the diameter approaches 0.5 μm. These times are typical of those used to acquire EDX and EELS spectra in modern analytical electron microscopes. Since the current trend in microchemical analysis is to employ higher accelerating voltages, higher beam currents and smaller probe sizes, displacement-rate gradient effects are likely to become an important problem for EDX and EELS. Due to the extremely small probe size employed by these techniques, significant changes during analysis may occur in many materials, even near room temperature.

Finally, the ability to locally modify the alloy composition, and the nature, density and distribution of precipitates by irradiation with highly-focused electron

beams may offer a new, efficient method for producing local regions of controlled composition and microstructure in thin films on a nanometer scale. Potential applications in the area of device fabrications for integrated circuits should be explored.

ACKNOWLEDGEMENTS

The authors are grateful to B. J. Kestel, E. A. Ryan and A. Philippides for their valuable technical assistance. Special thanks are extended to Mrs. D. Livengood for her skillful formatting and typing of the paper. This work was supported by the U. S. Department of Energy.

REFERENCES

1. L. Kaufman and H. Bernstein, Computer Calculations of Phase Diagrams, Academic Press, New York (1979).
2. K. Y. Liou and P. Wilkes, J. Nucl. Mater. 87, 317 (1979).
3. R. S. Nelson, J. A. Hudson and D. J. Mazey, J. Nucl. Mater. 44, 318 (1972).
4. S. I. Maydet and K. C. Russell, J. Nucl. Mater. 64, 101 (1977).
5. R. Sizmann, J. Nucl. Mater. 69 & 70, 386 (1979).
6. R. A. Johnson and N. Q. Lam, Phys. Rev. B 13, 4364 (1976).
7. R. A. Johnson and N. Q. Lam, J. Nucl. Mater. 69 & 70, 424 (1978).
8. N. Q. Lam, P. R. Okamoto and R. A. Johnson, J. Nucl. Mater. 78, 408 (1978).
9. P. R. Okamoto and L. E. Rehn, J. Nucl. Mater. 83, 2 (1979).
10. H. Wiedersich, P. R. Okamoto and N. Q. Lam, J. Nucl. mater. 83, 98 (1979).
11. H. Wiedersich and N. Q. Lam, in Phase Transformations during Irradiation, (edited by F. V. Nolfi, Jr.), p. 1. Applied Science Publishers, Essex (1983).
12. G. Martin, R. Cauvin and A. Barbu, in Phase Transformations during Irradiation, (edited by F. V. Nolfi, Jr.), p. 47. Applied Science Publishers, Essex (1983).
13. L. E. Rehn and P. R. Okamoto, in Phase Transformations during Irradiation, (edited by F. V. Nolfi, Jr.), p. 247. Applied Science Publishers, Essex (1983).
14. N. Q. Lam, K. Janghorban and A. J. Ardell, J. Nucl. Mater. 101, 314 (1981).
15. P. R. Okamoto, L. E. Rehn and R. S. Averback, J. Nucl. Mater. 108 & 109, 319 (1982).
16. N. Q. Lam, J. Nucl. Mater. 117, 106 (1983).
17. N. Q. Lam, G. K. Leaf and M. Minkoff, J. Nucl. Mater. 118, 248 (1983).
18. N. Q. Lam and P. R. Okamoto, in Effects of Radiation on Materials - Twelfth Symposium, (edited by F. A. Garner and J. S. Perrin), ASTM STP 870, p. 430. ASTM, Philadelphia, PA (1985).
19. P. R. Okamoto and N. Q. Lam, Mat. Res. Soc. Symp. Proc. 41, 241 (1985).
20. N. Q. Lam and P. R. Okamoto, J. Nucl. Mater. 133 & 134 (1985) in press.
21. C. W. Allen, P. R. Okamoto and N. J. Zaluzec, unpublished work.
22. K. Janghorban and A. J. Ardell, in Phase Stability during Irradiation, (edited by J. R. Holland et al.), p. 547. AIME, New York (1981).
23. A. J. Ardell and R. B. Nicholson, Acta Metall. 14, 1295 (1966).
24. T. Muroga and P. R. Okamoto, unpublished work.

No text below this line